DNA-based delivery of incretin receptor agonists using MYO Technology leads to durable weight loss in a diet-induced obesity model

Linda Sasset[1], Andrew Cameron[1], Carleigh Sussman1, Luisa Rubinelli[1], Debnath Maji[1,2], Robert Miller[1], Andy Thompson[1], Delcora Campbell[1], Melanie R. Walker[1], Marek M. Drozdz[1,*], Rachel A Liberatore[1,*]

[1]RenBio Inc., Long Island City, New York, NY 11101, USA.

[2] Department of Biological and Agricultural Engineering, Louisiana State University, Baton Rouge, LA 70803, USA

* Correspondence should be addressed to R.A.L. (rachel.liberatore@renbio.com) or M.M.D. (marek.drozdz@renbio.com)

ABSTRACT

Therapeutic proteins have seen a substantial increase in clinical development and use across many disease areas. Despite their broad applicability, significant drawbacks limit access to many of these drugs, including: i) high manufacturing costs; ii) administration via time-consuming infusions; iii) frequent dosing, sometimes even daily; and iv) requirements for low temperature storage.

MYO Technology was developed to overcome these barriers. The MYO Technology platform consists of therapeutic-encoding plasmid DNA (pDNA), and a proprietary medical device for intramuscular injection and delivery of electrical pulses. These pulses enable the *in vivo* electroporation of muscle cells and uptake of injected pDNA, leading to the production, secretion, and delivery of the therapeutic protein into peripheral circulation. MYO Technology offers several advantages over standard delivery of therapeutic proteins; pDNA manufacturing is a simpler and less specialized process compared to protein manufacturing,

and pDNA is very stable and lacks most cold chain requirements. Furthermore, administration using MYO Technology takes only a few minutes, and the serum level of a therapeutic protein can potentially be maintained for many months without the need for redosing.

Incretin receptor agonists (IRAs) are a class of therapeutic proteins that have recently come to prominence as powerful weight and glucose control drugs, and are used for the treatment of type 2 diabetes (T2D) and obesity. Semaglutide and tirzepatide, currently the most widely used within this class, are both potent molecules, but have a short half-life, requiring weekly administration by subcutaneous injections. Moreover, since their clinical benefits rapidly disappear upon treatment cessation, T2D and obese patients may have a life-long dependency on IRAs, and the requirement for weekly injections can negatively affect the quality of life and the adherence to therapy, as well as create a significant financial burden. Therefore, increasing the interval between injections has become one of the major goals in the field.

Here, we present our preclinical studies on the delivery of IRAs with MYO Technology. Animal proof-of-concept studies demonstrate that MYO Technology-delivered IRAs are functional, and efficacious in promoting long-lasting weight and glucose control in mouse models of diet-induced obesity. Moreover, engineering the IRAs to facilitate blood–brain barrier penetration further enhances treatment efficacy, with benefits persisting well beyond six months following a single administration. Together, these findings highlight MYO Technology's potential to transform care for patients with T2D and obesity by enabling long-lasting therapeutic effects with minimal dosing, ultimately improving quality of life and treatment adherence.

56 **INTRODUCTION**

57

58 Glucagon like peptide-1 (GLP-1) is an emerging glucose control and weight loss drug, which
59 is used in the treatment of type 2 diabetes (T2D) and obesity. This peptide is administered
60 subcutaneously to patients, and upon binding to its receptor in different organs, GLP-1
61 exerts several effects: in the pancreas it enhances insulin secretion and inhibits glucagon
62 release, in the stomach it delays gastric emptying, and in the hypothalamus it reduces
63 hunger, increases the feeling of satiety, and alters feeding behavior, overall decreasing body
64 weight and ameliorating metabolic dysregulation[1].
65 A significant downside of GLP-1 is its short half-life, which is about 2-5 minutes in vivo[2] .
66 Despite significant progress made in the field to incorporate modifications capable of
67 improving its durability, the current GLP-1 class of drugs used in the clinic still has a half-life
68 of only about one week, making weekly dosing necessary to maintain its therapeutic effects[3].
69 Several molecules are currently approved for both obesity and T2D: liraglutide (Saxenda) and
70 semaglutide (Ozempic/Wegovy) are GLP-1 receptor agonists, and tirzepatide
71 (Mounjaro/Zepbound) is a double GLP-1 and GIP receptor agonist. All of these molecules
72 have an added fatty acid moiety, which binds albumin as a mechanism for half-life
73 extension[4]. Some earlier generation molecules are only approved for T2D, such as
74 dulaglutide (Trulicity), which incorporates an Fc fusion as a strategy for half-life extension[5].
75 RenBio has evaluated intramuscular electroporation (IM-EP)-mediated delivery of plasmid
76 DNA (pDNA), encoding GLP-1, using its MYO (Make Your Own) Technology, as a new
77 therapeutic strategy. With this approach, GLP-1 is constantly produced for an extended
78 period, overcoming the necessity for weekly dosing. This technology has been successfully
79 employed in animal models of neutropenia for the delivery of granulocyte colony stimulating
80 factor (G-CSF), another small therapeutic protein with a short (~3.5 hours) half-life[6] .

81

82 MYO Technology takes advantage of the efficiency of in vivo transfection of skeletal muscle
83 cells enabled by EP, and the durable protein production by those cells following
84 transfection[7] . Indeed, expression of a monoclonal antibody or other therapeutic protein can

be sustained for several months to a year or more, both in animal models, and most importantly, in a clinical setting[6] . Because of this durability, the potential exists to make a significant impact on the treatment of chronic diseases, including obesity[7].

The GLP-1 class of drugs has recently transformed the treatment of obesity, though questions remain regarding the full suite of mechanisms of action of these molecules. In addition to direct action on the gastrointestinal tract, data suggest that targets in the brain are important for their activity[8]. Angiopep-2 is a peptide that has been shown to increase penetration of the blood-brain barrier (BBB) when fused to heterologous proteins[9] . Using a mouse model of diet-induced obesity (DIO), we demonstrate sustained weight loss and improved glucose metabolism for ~40 weeks following a single dose of a GLP-1-Fc fusion protein with an appended Angiopep-2 moiety. This approach raises the prospect of dramatically reduced dosing frequency of this important class of therapeutics.

RESULTS

DNA-based delivery of GLP-1 peptide is efficacious in a diet induced obesity model

To evaluate the feasibility of DNA-based delivery of GLP-1 with MYO Technology we used a DIO mouse model[10–12]. Recombinant GLP-1 currently used in clinic has an added fatty acid moiety, which binds albumin and aids in half-life extension[4] but this is incompatible with a DNA-based approach. We were able to alter the cleavage site recognized by DPP-4 in GLP-1, another strategy incorporated into the current class of GLP-1 drugs . DPP-4 is a protease that breaks down incretin hormones like GLP-1 and GIP, and plays a key role in the regulation of GLP-1 activity[13].

To evaluate the effect of MYO-delivered GLP-1, mice were fed a high fat diet (HFD) for 8 weeks, and then divided into four groups: two groups were kept on HFD and two groups switched to a standard diet (SD). We reasoned that the cohorts fed SD would better resemble a clinical scenario where obesity patients make dietary changes in addition to the drug treatment. Within each diet group, one subgroup was electroporated with the pDNA

114 encoding GLP-1 and one kept as a control (Figure 1A). Mice that remained on HFD and
115 received GLP-1 showed reduced weight gain in the first two weeks compared to the placebo
116 controls (Figure 1B). This effect was transient, and after 2 weeks, all animals on HFD gained
117 weight at the same rate. The therapeutic effect of MYO-delivered GLP-1 was much more
118 pronounced in mice switched to SD (Figure 1C). The experimental cohort started losing
119 weight immediately after IM-EP, showing over 15% weight loss compared to placebo control
120 by week 2. Between week 3 and 5, however, animals started regaining weight, and by the
121 end of the experiment, the placebo adjusted weight loss was at ~5%.
122 Another important effect of GLP-1 molecules is the improvement of glycemic control. We
123 therefore performed a glucose tolerance test (GTT) assay at different time points post IM-EP.
124 GTT is a test that measures how the body regulates blood sugar levels after consuming a
125 known amount of glucose[14]. Two weeks after IM-EP delivery, mice that received GLP-1
126 showed improved glucose clearance compared to controls in HFD groups (Figure 1D),
127 demonstrating that the MYO-delivered GLP-1 is biologically active. We also examined
128 glycemia at a later timepoint, when any weight loss benefit was already diminished. Not
129 surprisingly, at eight weeks after IM-EP, we did not detect any difference in the glucose
130 clearance rate (Figure 1E). The same was true for the animals switched to SD; two weeks after
131 EP, animals that received GLP-1 showed improved GTT, but the effect had disappeared by
132 week 8 (Figure 1F and G, respectively).
133
134 **GLP-1 fused to an Fc domain exhibits therapeutic effects comparable to those of**
135 **semaglutide**
136 Since the therapeutic effect of native GLP-1 peptide was limited in time, we decided to fuse
137 GLP-1 with the sequence encoding an IgG Fc region in order to extend the molecule's half-
138 life and boost its bioavailability[5]. We focused on a murine Fc sequence to allow proof-of-
139 concept studies in a DIO mouse model without evoking an anti-drug antibody response. The
140 encoded protein is referred to as GLP-1-mIgG1(Fc) (Figure 2A).
141 First, we compared the potency of GLP-1-mIgG1(Fc) with that of semaglutide. To do so, we
142 developed an in vitro reporter assay[15]. We co-expressed GLP-1 receptor (GLP-1R) and a

143 luciferase reporter under the control of a cAMP-responsive element (CRE) in HEK293T cells.
144 GLP-1R activation leads to the activation of the adenylyl cyclase and consequent increase in
145 cAMP generation which, in turn, activates CRE-dependent transcription. Using this assay, we
146 evaluated GLP-1R activation by recombinant GLP-1-mIgG1(Fc) or semaglutide (Figure 2B). We
147 determined semaglutide EC50 at 0.29 nM, which is comparable to 0.15 nM reported by Novo
148 Nordisk in their FDA application (application #210913Orig1s000). GLP-1-mIgG1(Fc), albeit
149 less potent than semaglutide, activated GLP-1R at low nanomolar ranges (EC50 = 7.35 nM).
150 Next, we evaluated GLP-1-mIgG1(Fc) compared to semaglutide in DIO mice when delivered
151 as purified protein, instead of IM-EP of pDNA. We followed the same diet protocol described
152 in Figure 1A. After randomization into HFD and SD groups, animals received either molecule
153 subcutaneously at 30nmol/kg over a period of 10 days, then observed for another 11 days
154 to monitor the effects of drug withdrawal.
155 In both HFD and SD groups, GLP-1-mIgG1(Fc) and semaglutide demonstrated comparable: i)
156 reduction of body weight (Figure 2C and D, top panels); ii) weight rebound post-withdrawal
157 (Figure 2C and D, bottom panels); and iii) improved glucose clearance (Figure 2E and F). These
158 data confirm that the GLP-1 Fc fusion and semaglutide have comparable effects on weight
159 and glucose metabolism in mice.
160
161 **DNA-based delivery of GLP-1 Fc fusion improves weight loss compared to native GLP-1**
162 After confirming comparable potency of recombinant GLP-1-mIgG(Fc) and semaglutide, we
163 delivered DNA-encoded GLP-1-mIgG1(Fc) with MYO Technology, following the same diet
164 protocol as before (Figure 1A). Similar to the first study (Figure 1B), the cohort kept on a HFD
165 lost minimal weight compared to controls (Figure 3A). The cohort switched to SD, however,
166 started losing weight immediately after EP and showed much bigger weight loss than GLP-1
167 alone (Figure 3B). Importantly, even after animals started regaining weight past week 3, the
168 placebo adjusted weight loss remained at ~10% by the end of the experiment at week 6,
169 which was a two-fold improvement from the GLP-1 alone. Assessment of the GTT showed a
170 significant improvement in the glycemic control in groups that received GLP-1 Fc fusion. The

171 difference was significant at 2 weeks after EP regardless of the diet, and was maintained at
172 week 6 in the SD cohort (Figure 3C-F).
173
174 **Enhanced BBB crossing dramatically improves GLP-1-mIgG1(Fc) efficacy**
175 One of the mechanisms by which GLP-1 promotes weight loss is by binding to GLP-1R in the
176 brain, particularly in the hypothalamus, and enhancing the feeling of satiety[1,16]. GLP-1-
177 mIgG1(Fc) fusion is a relatively large protein and presumably unable to easily penetrate the
178 BBB. The inability to pass through the BBB is an issue for several large molecules (e.g.
179 antibodies) as well as for adeno-associated viral vectors, and several strategies have been
180 recently developed to overcome this. One such strategy is the addition of Angiopep-2, a 19
181 amino acid peptide that binds to the low-density lipoprotein receptor related protein-1 (LRP-
182 1) expressed by the endothelial cells of the BBB; Angiopep-2 binding to LRP-1 facilitates the
183 transcytosis of the molecules conjugated to the peptide[17,18]. Therefore, we decided to assess
184 whether the addition of Angiopep-2 to GLP-1-mIgG1(Fc) could improve the molecule's
185 efficacy in treatment of obesity. This new molecule is referred to as GLP-1-mIgG1(Fc)-Angp2
186 (Figure 4A).
187 First, we evaluated the potency of GLP-1-mIgG1(Fc)-Angp2 on GLP-1R and compared it to
188 that of semaglutide and GLP-1-mIgG1(Fc), using the in vitro reporter assay described earlier
189 in this manuscript. While addition of Angiopep-2 to GLP-1-mIgG1(Fc) led to reduction of the
190 potency, it remained at a low EC50 of 31.1 nM (Figure 4B). Thus, we decided to evaluate DNA-
191 based delivery of this molecule in the DIO model, following the same diet protocol described
192 in Figure 1A. Mice that remained on HFD lost ~7% placebo adjusted weight in the first 2
193 weeks, and for the following 16 weeks they gained weight at a slower rate compared to
194 controls (Figure 4C), but the weight started rebounding after week 18. Mice switched to SD,
195 however, exhibited a much more robust therapeutic effect of GLP-1-mIgG1(Fc)-Angp2 after
196 MYO delivery. They started losing weight immediately after IM-EP with ~15% placebo
197 adjusted weight reduction, sustained for over 9 months after a single administration (Figure
198 4D). We also assessed the response to glucose via GTT assay at different time points.
199 Importantly, mice that received DNA-encoded GLP-1-mIgG1(Fc)-Angp2 showed an improved

200 glucose clearance compared to the controls over an extended period (Figure 4E and F). The
201 effect in animals on SD was more durable, and at week 45 still significantly differentiated
202 from placebo. Interestingly, in the HFD cohort, by week 24 no difference in GTT was detected
203 between treated and control animals, which correlated with weight rebound in the treated
204 animals. These data suggest that targeting GLP-1-mIgG1(Fc) to the BBB, thereby enabling
205 access to hypothalamic GLP-1R, is critical for sustained weight loss and long-term glucose
206 control.
207
208 **Human Fc fusion demonstrates similar effects in an obesity model**
209 Given the ultimate goal of developing a molecule suitable for clinical use, we replaced the
210 murine IgG1 Fc domain with that of human IgG4, and retained the Angiopep-2 fusion. This
211 molecule is referred to as GLP-1-hIgG4(Fc)-Angp2 (Figure 5A).
212 First, we evaluated the potency of GLP-1-hIgG4(Fc)-Angp2 on GLP-1R and compared it to the
213 potency of semaglutide, as described before. We determined that GLP-1-hIgG4(Fc)-Angp2
214 binds GLP-1R and exhibits low EC_{50} of 4.3 nM (Figure 5B).
215 We then evaluated the delivery of GLP-1-hIgG4(Fc)-Angp2 with MYO Technology in mice,
216 following the same experimental design as before (Figure 1A). Mice that were administered
217 DNA-encoded GLP-1-hIgG4(Fc)-Angp2 and kept on a HFD gained weight at a slower rate
218 compared to controls, showing ~7% placebo adjusted weight loss (Figure 5C). Mice that were
219 switched to SD showed over 10% placebo adjusted weight loss (Figure 5D). Furthermore, GTT
220 tests performed at week 4 showed a significantly improved glucose clearance compared to
221 control, regardless of the diet (Figure 5E and 5G). The effect in animals on SD was maintained
222 also at week 12, while in the HFD cohort, at week 12 no difference in GTT was detected
223 between treated and control animals, which correlated with weight rebound in the treated
224 animals (Figure 5F and 5H).
225 These data are consistent with our hypothesis that targeting a GLP-1Fc fusion to the brain
226 via the addition of Angiopep-2 promotes a sustained weight loss and a better glucose
227 clearance over time.
228

229 **MATERIAL AND METHODS**

230

231 **Animals**

232 All animal procedures were performed at Mispro facilities and overseen by the Mispro
233 Institutional Animal Care and Use Committee (IACUC), with the animals cared for in
234 accordance with all federal and state regulations. The mice were housed in disposable,
235 individually ventilated, filter-top cages (Innocage®, Innovive Inc., San Diego, CA, USA).
236 6/8-week-old C57BL/6J (The Jackson Laboratory, strain #000664) male mice were fed high fat
237 diet (HFD. ResearchDiet, cat# D12451) for 8 weeks. The day before study initiation all mice
238 were weighed and randomized into treatment groups based on body weight (BW) so that all
239 groups had similar starting BW before treatment (n = 5/group). Immediately after IM/EP,
240 mice were either kept on HFD or switched to a standard diet (SD. ResearchDiet, cat#
241 D12450H), and monitored as indicated in the result section. During the course of the study
242 mice weight was recorded weekly. For the % of weight gain/loss (top panels), individual
243 mouse weight recorded the day before IM/EP was considered 100%, and the weight at the
244 following time-points calculated relative to this 100% baseline. For weight loss placebo
245 adjusted, for each week the mouse average weight in the control cohort was considered
246 100%. Then, the individual weights in the treated cohort calculated as a percentage of this
247 100% baseline. The difference between this percentage and 100% represents the percentage
248 of weight loss compared to the placebo group.

249

250 **Electroporation**

251 Electroporation was performed bilaterally in the tibialis anterior (TA) muscle. Target muscle
252 was injected with a 40 µL mixture consisting in 50 µg of pDNA and 3U of Hylenex®
253 (hyaluronidase human injection, Halozyme Therapeutics), formulated in 0.45% saline, with
254 pDNA at a final concentration of 1.25 µg/µL. This formulation was injected using a 29-gauge
255 syringe (Becton Dickinson, cat# 324702), at a depth of 1.9 ± 0.2 mm. The pDNA injection was
256 immediately followed by electroporation using an in-house-developed needle-based
257 electroporator. The electroporator consists of four 0.3 mm diameter gold acupuncture

258 needle electrodes (Asiamed, cat# AMG-3030), each at the corner of a 2 × 2 mm square. A
259 series of pulses at 150 V/cm was applied using a RenBio custom-built generator (RenBio Inc).
260
261 **Glucose Tolerance Test (GTT)**
262 After overnight fasting, basal glucose levels were recorded by using an Auvon glucose meter.
263 Mice were then injected with a glucose (Sigma-Aldrich, cat# G7021) solution intraperitoneally
264 (1.5 g/kg BW in water) and blood glucose measured at the indicated times.
265
266 **GLP-1R in vitro reporter assays**
267 HEK293T (cat#) were seeded at 1.8e6 cells in a 10 cm plate in DMEM (Corning, cat# 10-017-
268 CV) completed with 10% FBS (Corning, cat# 35-011-CV) and 1x pen/strep (Corning 30-002-CI).
269 After 24h 2.5 ug of pDNA expressing GLP-1R and 2.5 ug of pGL4.29[*luc2P*/CRE/Hygro]
270 (Promega, cat# E8471) were transiently transfected with PEI. DNA encoding GLP-1R
271 (GenBank, Gene ID: 2740) was cloned into the pCBAINA, a gWiz-derived expression construct.
272 The backbone of pCBAINA includes a cytomegalovirus (CMV) enhancer, chicken beta actin
273 promoter, CMV intron A, bovine growth hormone polyadenylation (BGH-PolyA) sequence,
274 and kanamycin resistance gene. GLP-1R sequence was synthesized by Twist Bioscience (San
275 Francisco, CA, USA). Medium was changed 6h post-transfection to selection medium
276 containing 0.5 ug/mL of puromycin (Boston Bioproducts, cat# ABT-440). 24h post-
277 transfection cells were seeded at 70000/well in a 96 multiwell plate. 48h post-transfection
278 cells were incubated with different concentrations of IRAs. After 3h of incubation cells were
279 lysed with Bright-Glo™ Luciferase Assay System (Promega, cat# E2610) according to the
280 manufacturer's protocol, and the luminescence was measured using GloMax Navigator
281 Microplate Luminometer (Promega, cat# GM2000). Luminescence data were normalized as
282 % activation compared to the one of semaglutide at the maximum concentration.
283
284

285 **DISCUSSION**

286 In recent years, the IRA class of drugs such as GLP-1 have transformed the treatment of
287 obesity and T2D[3] . It is clear that these molecules not only have the potential to help patients
288 lose weight, but also to make inroads in tackling many of the comorbidities associated with
289 these diseases, including cardiovascular and kidney diseases[19–21]. A major drawback to these
290 drugs, however, is their relatively short half-life, despite both genetic and biochemical
291 modifications aimed at improving their pharmacokinetic (PK) profile. Because of this, the
292 majority of the current generation of approved GLP-1 drugs must be dosed weekly by
293 subcutaneous injection. And as a result of the expense associated with manufacturing
294 protein biologics, as well as the frequent dosing regimen required, these drugs can exact a
295 high cost from patients, often in the range of $1000 per month.

296 In order to address these barriers of frequent dosing and high costs, we have evaluated a
297 DNA-based delivery approach. Previous work with our MYO Technology platform for the
298 delivery of another small therapeutic protein with a short half-life, G-CSF, yielded very
299 encouraging results regarding the ability of this approach to overcome the poor PK profile
300 of some small proteins[6] . Given these results, we sought to determine if this approach could
301 similarly improve the outcomes of treatment with IRAs.

302 We found that delivery of a GLP-1 RA alone could indeed lead to weight loss in a mouse DIO
303 model. However, these effects were transient, and only significantly different from untreated
304 controls when the animals were also switched to a standard diet following treatment. In
305 order to probe the effect of modifications that would improve the half-life of these
306 molecules, we generated and evaluated Fc-fusion variants, initially appending a murine IgG1
307 Fc. This Fc-fusion protein demonstrated a modest improvement in both weight loss and
308 glucose metabolism as compared to the unmodified GLP-1 RA molecule.

309 Though questions remain about the various mechanisms by which the GLP-1 class of
310 molecules exert their effects on weight loss, strong data indicate that targets in the brain
311 play a role[1] . Thus, we sought to understand whether increased access to the brain, via

312 improved penetration of the BBB, may lead to improved efficacy. Indeed, by appending
313 Angiopep-2, a peptide known to increase BBB targeting[9] , we significantly improved the
314 magnitude and duration of weight loss following a single administration, an effect that
315 persisted for over 40 weeks. This was also accompanied by a durable improvement in
316 glucose metabolism. Importantly, this effect was also apparent in the context of a human
317 IgG1 fusion, though this study has not yet been followed as long.

318 These results clearly demonstrate that the addition of Angiopep-2 to a GLP-1 RA improves
319 both the magnitude and durability of weight loss in a mouse DIO model, when delivered as
320 a DNA-based drug with MYO Technology. In order to further probe the mechanism of this
321 effect, we plan to evaluate the biodistribution of this new molecule, with a particular focus
322 on the central nervous system.

323 Although the GLP-1 class of drugs has clearly demonstrated potency in terms of overall
324 weight loss, improving the quality of weight loss remains one of the next important hurdles.
325 Many groups are evaluating the ability of additional therapeutics to reduce lean muscle loss,
326 primarily in the form of monoclonal antibodies targeting pathways involved in muscle
327 maintenance and growth, such as myostatin or activin[22,23] . MYO Technology-based delivery
328 is particularly well-suited to such multiplexing, in that delivery of multiple genes can be easily
329 accomplished either on a single plasmid or via incorporation of multiple plasmids expressing
330 different genes.

331 GLP-1 drugs have ignited a dramatic shift in obesity research and treatment, revealing both
332 impressive efficacy and areas clearly needing improvement. We have demonstrated that a
333 DNA-based delivery approach, using MYO Technology, has the potential to overcome the
334 poor PK profile associated with these drugs. Additionally, by taking advantage of the ease of
335 co-delivery of multiple biologics using this approach, we present an opportunity to evaluate
336 many of the molecules aimed at improving the quality of weight loss achieved by these
337 remarkable drugs.

338

FIGURES

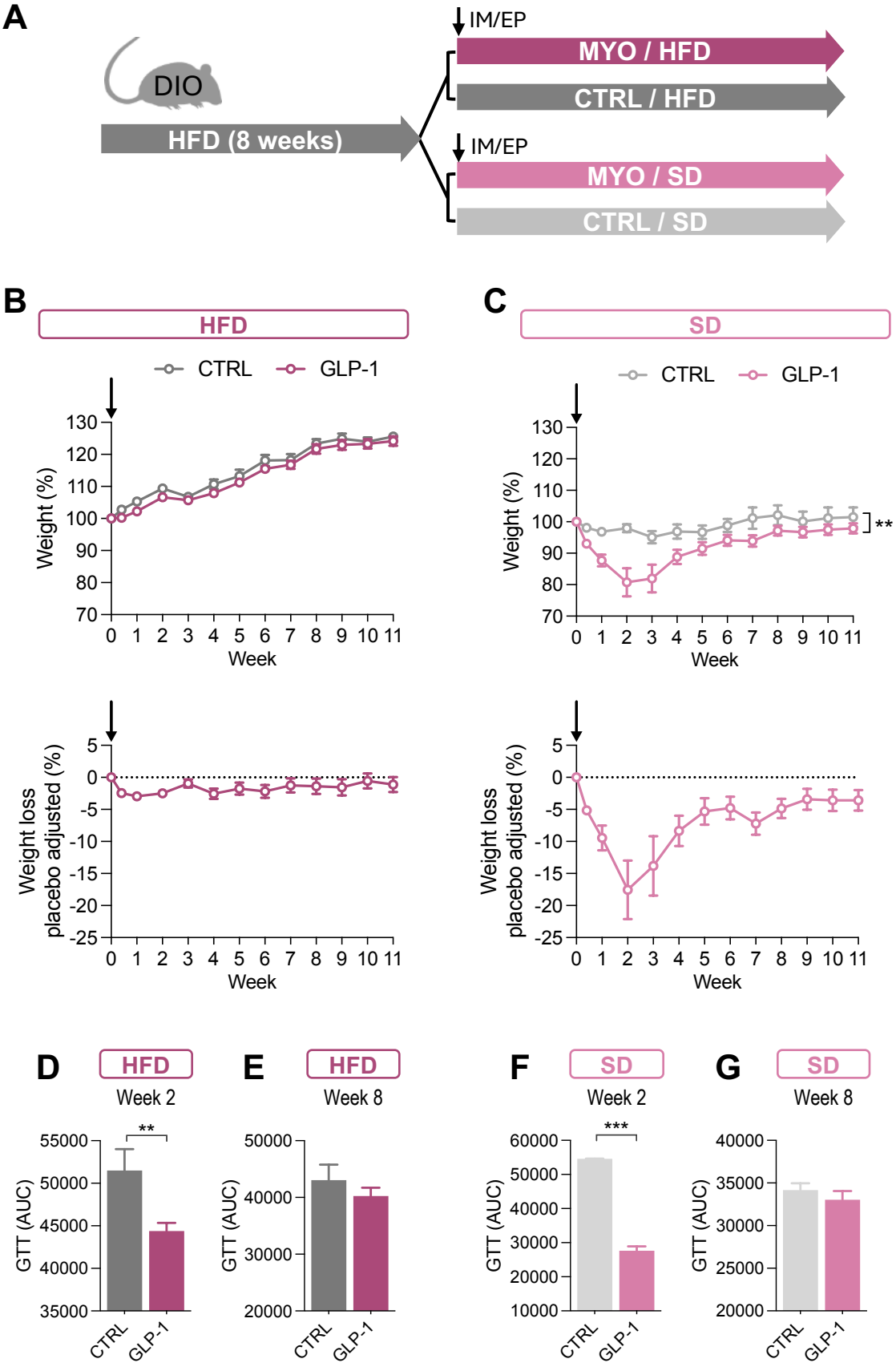
A
DIO
HFD (8 weeks)
IM/EP
MYO / HFD
CTRL / HFD
IM/EP
MYO / SD
CTRL / SD
B
HFD
CTRL
GLP-1
Weight (%)
Week
Weight loss placebo adjusted (%)
C
SD
CTRL
GLP-1
Weight (%)
Week
**
Weight loss placebo adjusted (%)
D
HFD
Week 2
**
GTT (AUC)
CTRL
GLP-1
E
HFD
Week 8
GTT (AUC)
CTRL
GLP-1
F
SD
Week 2
***
GTT (AUC)
CTRL
GLP-1
G
SD
Week 8
GTT (AUC)
CTRL
GLP-1

341 **Figure 1. DNA-based delivery of GLP-1 peptide is efficacious in a diet induced obesity**
342 **model. (A)** Experimental design. Percentage of absolute (top panel) and placebo adjusted
343 weight gain/loss (bottom panel) relative to the time of the EP (Week 0) in mice fed **(B)** high
344 fat diet (HFD) (n=5), and **(C)** standard diet (SD) (n=5). Area under the curve (AUC) derived from
345 glucose tolerance test (GTT) performed at **(D)** week 2, and **(E)** week 8 in mice fed HFD (n=5).
346 AUC derived from GTT performed at **(F)** week 2, and **(G)** week 8 in mice fed SD (n=5). Data
347 are expressed as mean ± SEM. ** $p<0.01$, *** $p<0.01$. Statistical significance was determined
348 by Two-way mixed-effects ANOVA (**B-C**) and unpaired t-test (**D-G**).
349

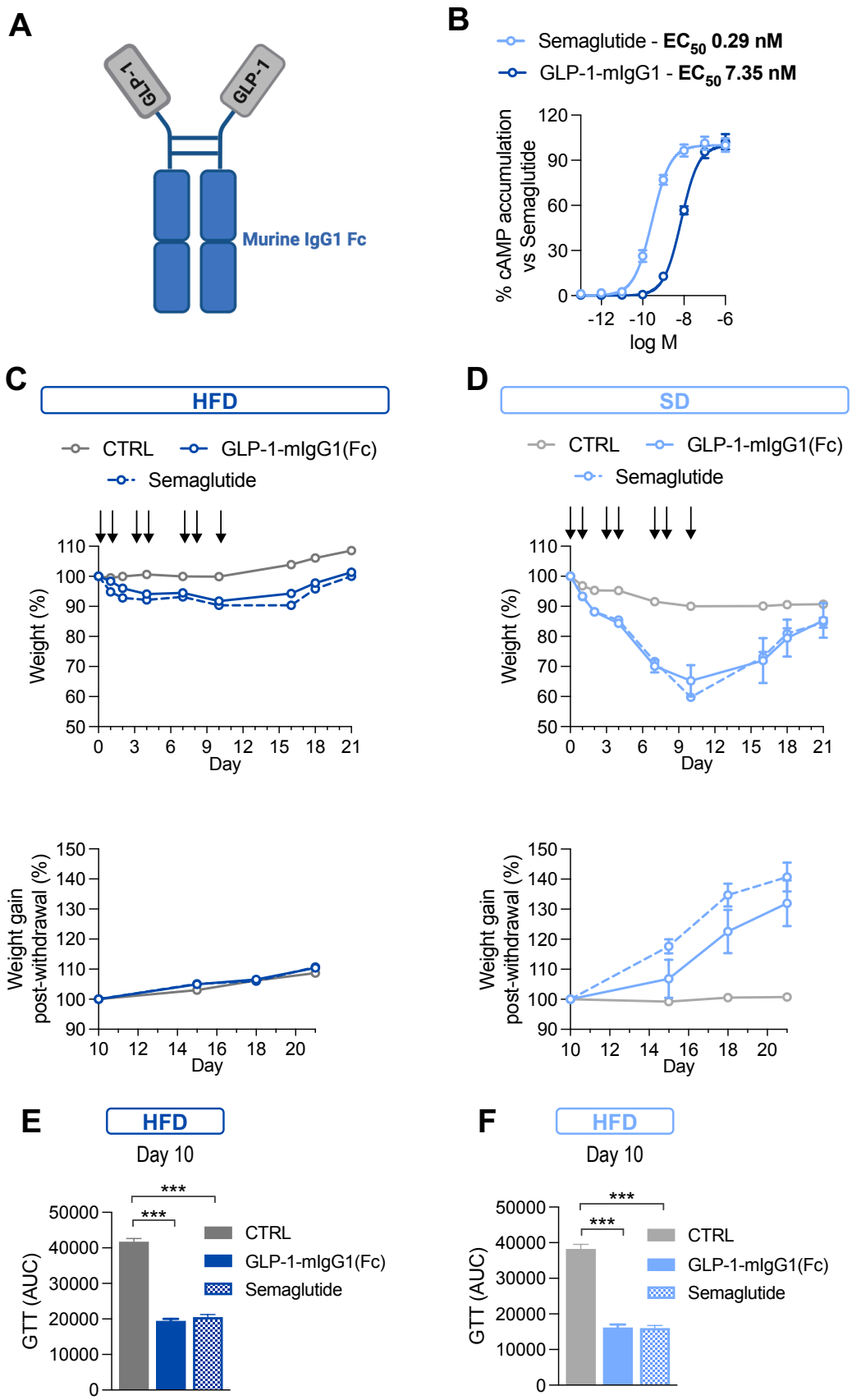
A
GLP-1
GLP-1
Murine IgG1 Fc
B
Semaglutide - EC50 0.29 nM
GLP-1-mIgG1 - EC50 7.35 nM
% cAMP accumulation vs Semaglutide
log M
C
HFD
CTRL
GLP-1-mIgG1(Fc)
Semaglutide
Weight (%)
Day
Weight gain post-withdrawal (%)
Day
D
SD
CTRL
GLP-1-mIgG1(Fc)
Semaglutide
Weight (%)
Day
Weight gain post-withdrawal (%)
Day
E
HFD
Day 10
GTT (AUC)
CTRL
GLP-1-mIgG1(Fc)
Semaglutide
F
HFD
Day 10
GTT (AUC)
CTRL
GLP-1-mIgG1(Fc)
Semaglutide

351 **Figure 2. GLP-1 fused to an Fc domain exhibits therapeutic effects comparable to those**
352 **of semaglutide. (A)** Schematic of the protein. **(B)** Intracellular cAMP accumulation measured
353 in HEK293T cells expressing GLP-1R. Data are expressed as % of cAMP relative to the highest
354 semaglutide concentration (n=10 from 3 independent experiments). Percentage of absolute
355 weight gain/loss relative to the time of the first injection (Day 0, top panel), and percentage
356 of absolute weight gain relative to the time of the last injection (Day 10, bottom panel) in
357 mice fed **(C)** HFD (n=5), and **(D)** SD (n=5). Area under the curve (AUC) derived from glucose
358 tolerance test (GTT) performed at day 10 in mice fed **(E)** HFD (n=5), or **(F)** SD (n=5). Data are
359 expressed as mean ± SEM. *** $p<0.01$. Statistical significance was determined by One-way
360 ANOVA (**E-F**).
361

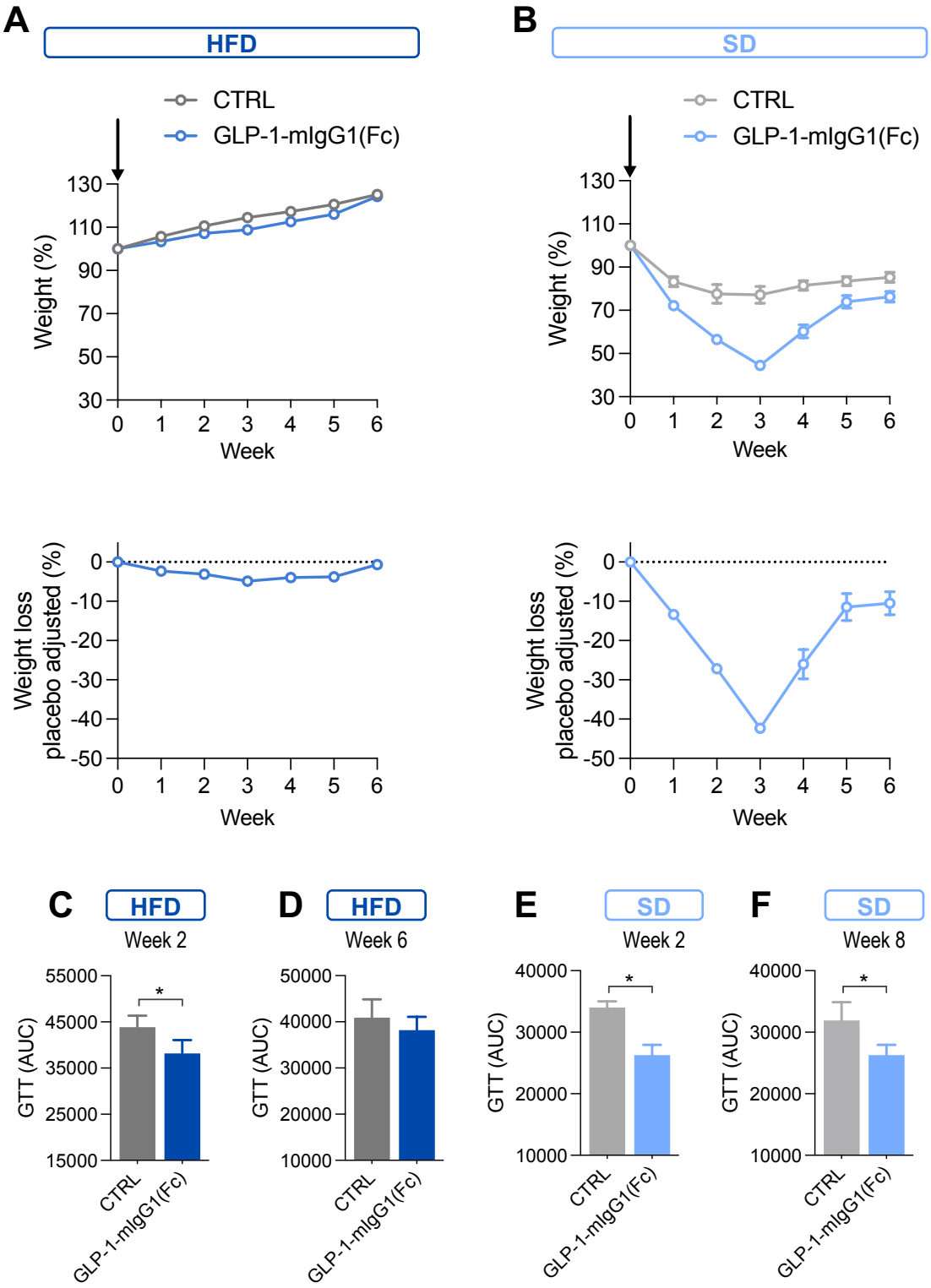

Figure 3. DNA-based delivery of GLP-1 Fc fusion improves weight loss compared to native GLP-1. Percentage of absolute (top panel) and placebo adjusted weight gain/loss (bottom panel) relative to the time of the EP (Week 0) in mice fed in mice fed **(B)** HFD (n=5),

366 and **(C)** SD (n=5). Area under the curve (AUC) derived from glucose tolerance test (GTT)
367 performed at **(C)** week 2, and **(D)** week 6 in mice fed HFD (n=5), and at **(E)** week 2, and **(F)**
368 week 6 in mice fed SD (n=5). Data are expressed as mean ± SEM. * $p<0.05$. Statistical
369 significance was determined by unpaired t-test (**C-F**).
370

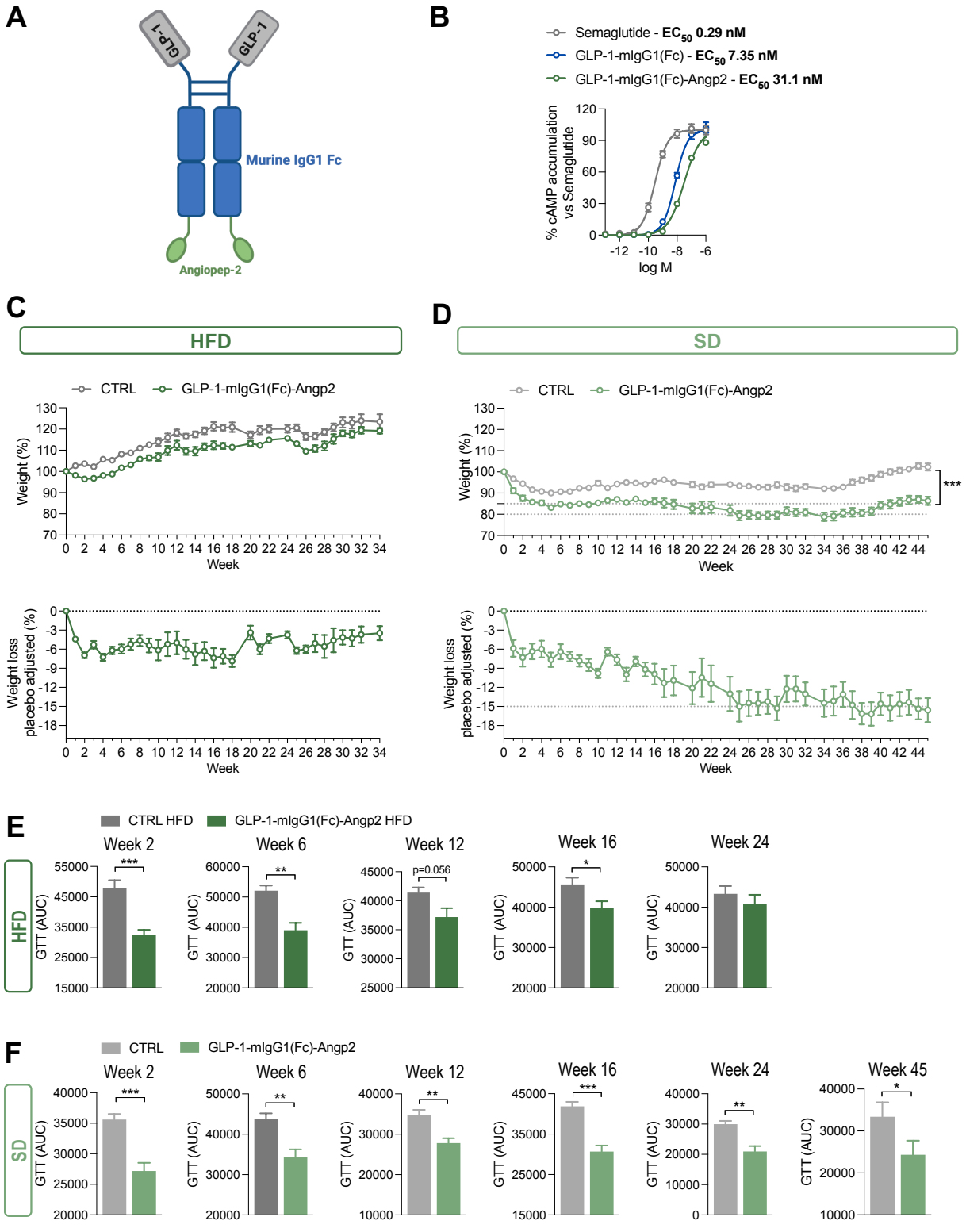

Figure 4. Enhanced BBB crossing dramatically improves GLP-1-mIgG1(Fc) efficacy. (A) Schematic of the protein. **(B)** Intracellular cAMP accumulation measured in HEK293T cells

374 expressing GLP-1R. Data are expressed as % of cAMP relative to the highest semaglutide
375 concentration (n≥4 from 3 independent experiments). Percentage of absolute (top panel)
376 and placebo adjusted weight gain/loss (bottom panel) relative to the time of the EP (Week 0)
377 in mice fed **(C)** high fat diet (HFD) (n=5), and **(D)** standard diet (SD) (n=5). Area under the
378 curve (AUC) derived from glucose tolerance test (GTT) performed at the time points indicated
379 in the figure in mice fed **(E)** HFD (n=5), or **(F)** SD (n=5). Data are expressed as mean ± SEM. *
380 p<0.05, ** p<0.01, *** p<0.01. Statistical significance was determined by Two-way mixed-
381 effects ANOVA (**C-D**) and unpaired t-test (**E-F**).
382

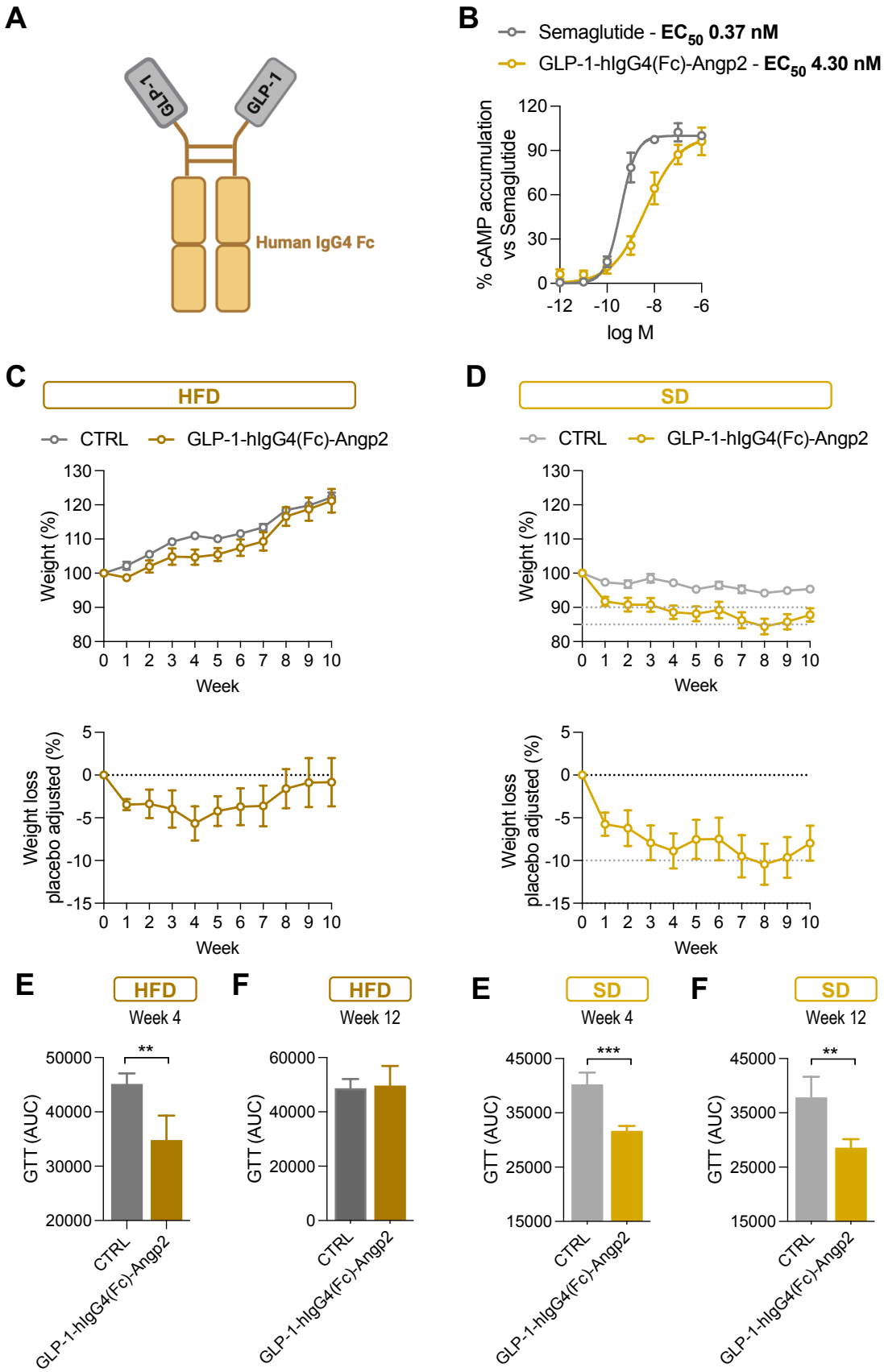
A
GLP-1
GLP-1
Human IgG4 Fc
B
Semaglutide - EC50 0.37 nM
GLP-1-hIgG4(Fc)-Angp2 - EC50 4.30 nM
% cAMP accumulation vs Semaglutide
log M
C
HFD
CTRL
GLP-1-hIgG4(Fc)-Angp2
Weight (%)
Week
Weight loss placebo adjusted (%)
D
SD
E
HFD
Week 4
F
HFD
Week 12
E
SD
Week 4
F
SD
Week 12
GTT (AUC)
CTRL
GLP-1-hIgG4(Fc)-Angp2

384 **Figure 5. Human Fc fusion demonstrates similar effects in an obesity model. (A)**
385 Schematic of the protein. **(B)** Intracellular cAMP accumulation measured in HEK293T cells
386 expressing GLP-1R. Data are expressed as % of cAMP relative to the highest semaglutide
387 concentration (n=3). Percentage of absolute (top panel) and placebo adjusted weight
388 gain/loss (bottom panel) relative to the time of the EP (Week 0) in mice fed **(C)** high fat diet
389 (HFD) (n=5), and **(D)** standard diet (SD) (n=5). Area under the curve (AUC) derived from
390 glucose tolerance test (GTT) performed at **(E)** week 4, and **(F)** week 12 in mice fed HFD (n=5),
391 and at **(G)** week 4, and **(H)** week 12 in mice fed SD (n=5). Data are expressed as mean ± SEM.
392 ** $p<0.01$, *** $p<0.01$. Statistical significance was determined by unpaired t-test (**E-G**).
393
394
395 **REFERENCES**

396 1. Zheng, Z., Zong, Y., Ma, Y., Tian, Y., Pang, Y., Zhang, C., and Gao, J. (2024). Glucagon-like
397 peptide-1 receptor: mechanisms and advances in therapy. Signal Transduct. Target. Ther. *9*,
398 234. https://doi.org/10.1038/s41392-024-01931-z.

399 2. Sharma, D., Verma, S., Vaidya, S., Kalia, K., and Tiwari, V. (2018). Recent updates on GLP-1
400 agonists: Current advancements & challenges. Biomed. Pharmacother. *108*, 952–962.
401 https://doi.org/10.1016/j.biopha.2018.08.088.

402 3. Friedman, J.M. (2024). The discovery and development of GLP-1 based drugs that have
403 revolutionized the treatment of obesity. Proc. Natl. Acad. Sci. *121*, e2415550121.
404 https://doi.org/10.1073/pnas.2415550121.

405 4. Bech, E.M., Pedersen, S.L., and Jensen, K.J. (2018). Chemical Strategies for Half-Life
406 Extension of Biopharmaceuticals: Lipidation and Its Alternatives. ACS Med. Chem. Lett. *9*,
407 577–580. https://doi.org/10.1021/acsmedchemlett.8b00226.

408 5. Glaesner, W., Vick, A.M., Millican, R., Ellis, B., Tschang, S., Tian, Y., Bokvist, K., Brenner, M.,
409 Koester, A., Porksen, N., et al. (2010). Engineering and characterization of the long-acting

410 glucagon-like peptide-1 analogue LY2189265, an Fc fusion protein. DiabetesMetab. Res. Rev.
411 *26*, 287–296. https://doi.org/10.1002/dmrr.1080.

412 6. Drozdz, M.M., Thompson, A.T., Sasset, L., Cameron, A.D., Yao, X., Maji, D., Campbell, D.A.,
413 Sussman, C., Miller, R., and Liberatore, R.A. (2025). DNA-based delivery of G-CSF as a durable
414 and efficacious approach to treat severe chronic neutropenia. Mol. Ther.
415 https://doi.org/10.1016/j.ymthe.2025.03.038.

416 7. Sussman, C., Liberatore, R.A., and Drozdz, M.M. (2024). Delivery of DNA-Based
417 Therapeutics for Treatment of Chronic Diseases. Pharmaceutics *16*, 535.
418 https://doi.org/10.3390/pharmaceutics16040535.

419 8. Baggio, L.L., and Drucker, D.J. (2014). Glucagon-like peptide-1 receptors in the brain:
420 controlling food intake and body weight. J. Clin. Investig. *124*, 4223–4226.
421 https://doi.org/10.1172/jci78371.

422 9. Li, Y., Zheng, X., Gong, M., and Zhang, J. (2016). Delivery of a peptide-drug conjugate
423 targeting the blood brain barrier improved the efficacy of paclitaxel against glioma.
424 Oncotarget *7*, 79401–79407. https://doi.org/10.18632/oncotarget.12708.

425 10. Bossart, M., Wagner, M., Elvert, R., Evers, A., Hübschle, T., Kloeckener, T., Lorenz, K.,
426 Moessinger, C., Eriksson, O., Velikyan, I., et al. (2022). Effects on weight loss and glycemic
427 control with SAR441255, a potent unimolecular peptide GLP-1/GIP/GCG receptor triagonist.
428 Cell Metab *34*, 59-74.e10. https://doi.org/10.1016/j.cmet.2021.12.005.

429 11. Coskun, T., Urva, S., Roell, W.C., Qu, H., Loghin, C., Moyers, J.S., O'Farrell, L.S., Briere, D.A.,
430 Sloop, K.W., Thomas, M.K., et al. (2022). LY3437943, a novel triple glucagon, GIP, and GLP-1
431 receptor agonist for glycemic control and weight loss: From discovery to clinical proof of
432 concept. Cell Metab *34*, 1234-1247.e9. https://doi.org/10.1016/j.cmet.2022.07.013.

433 12. Benichou, O., Coskun, T., Gonciarz, M.D., Garhyan, P., Adams, A.C., Du, Y., Dunbar, J.D.,
434 Martin, J.A., Mather, K.J., Pickard, R.T., et al. (2023). Discovery, development, and clinical proof
435 of mechanism of LY3463251, a long-acting GDF15 receptor agonist. Cell Metab *35*, 274-
436 286.e10. https://doi.org/10.1016/j.cmet.2022.12.011.

437 13. Mulvihill, E.E., and Drucker, D.J. (2014). Pharmacology, Physiology, and Mechanisms of
438 Action of Dipeptidyl Peptidase-4 Inhibitors. Endocr. Rev. *35*, 992–1019.
439 https://doi.org/10.1210/er.2014-1035.

440 14. Phillips, P.J. (2012). Oral glucose tolerance testing. Aust. Fam. physician *41*, 391–393.

441 15. Willard, F.S., Douros, J.D., Gabe, M.B.N., Showalter, A.D., Wainscott, D.B., Suter, T.M.,
442 Capozzi, M.E., Velden, W.J.C. van der, Stutsman, Cynthia., Cardona, G.R., et al. (2020).
443 Tirzepatide is an imbalanced and biased dual GIP and GLP-1 receptor agonist. JCI Insight *5*,
444 e140532. https://doi.org/10.1172/jci.insight.140532.

445 16. Pannacciulli, N., Le, D.S.N.T., Salbe, A.D., Chen, K., Reiman, E.M., Tataranni, P.A., and
446 Krakoff, J. (2007). Postprandial glucagon-like peptide-1 (GLP-1) response is positively
447 associated with changes in neuronal activity of brain areas implicated in satiety and food
448 intake regulation in humans. NeuroImage *35*, 511–517.
449 https://doi.org/10.1016/j.neuroimage.2006.12.035.

450 17. Demeule, M., Régina, A., Ché, C., Poirier, J., Nguyen, T., Gabathuler, R., Castaigne, J.-P., and
451 Béliveau, R. (2008). Identification and Design of Peptides as a New Drug Delivery System for
452 the Brain. J. Pharmacol. Exp. Ther. *324*, 1064–1072. https://doi.org/10.1124/jpet.107.131318.

453 18. Demeule, M., Currie, J., Bertrand, Y., Ché, C., Nguyen, T., Régina, A., Gabathuler, R.,
454 Castaigne, J., and Béliveau, R. (2008). Involvement of the low-density lipoprotein receptor-
455 related protein in the transcytosis of the brain delivery vector Angiopep-2. J. Neurochem.
456 *106*, 1534–1544. https://doi.org/10.1111/j.1471-4159.2008.05492.x.

457 19. Ferhatbegović, L., Mršić, D., and Macić-Džanković, A. (2023). The benefits of GLP1
458 receptors in cardiovascular diseases. Front. Clin. Diabetes Healthc. *4*, 1293926.
459 https://doi.org/10.3389/fcdhc.2023.1293926.

460 20. Badve, S.V., Bilal, A., Lee, M.M.Y., Sattar, N., Gerstein, H.C., Ruff, C.T., McMurray, J.J.V.,
461 Rossing, P., Bakris, G., Mahaffey, K.W., et al. (2025). Effects of GLP-1 receptor agonists on
462 kidney and cardiovascular disease outcomes: a meta-analysis of randomised controlled
463 trials. Lancet Diabetes Endocrinol. *13*, 15–28. https://doi.org/10.1016/s2213-8587(24)00271-
464 7.

465 21. Muskiet, M.H.A., Tonneijck, L., Smits, M.M., Baar, M.J.B. van, Kramer, M.H.H., Hoorn, E.J.,
466 Joles, J.A., and Raalte, D.H. van (2017). GLP-1 and the kidney: from physiology to
467 pharmacology and outcomes in diabetes. Nat. Rev. Nephrol. *13*, 605–628.
468 https://doi.org/10.1038/nrneph.2017.123.

469 22. Nunn, E., Jaiswal, N., Gavin, M., Uehara, K., Stefkovich, M., Drareni, K., Calhoun, R., Lee, M.,
470 Holman, C.D., Baur, J.A., et al. (2024). Antibody blockade of activin type II receptors preserves
471 skeletal muscle mass and enhances fat loss during GLP-1 receptor agonism. Mol. Metab. *80*,
472 101880. https://doi.org/10.1016/j.molmet.2024.101880.

473 23. Mastaitis, J.W., Gomez, D., Raya, J.G., Li, D., Min, S., Stec, M., Kleiner, S., McWilliams, T.,
474 Altarejos, J.Y., Murphy, A.J., et al. (2025). GDF8 and activin A blockade protects against GLP-
475 1–induced muscle loss while enhancing fat loss in obese male mice and non-human
476 primates. Nat. Commun. *16*, 4377. https://doi.org/10.1038/s41467-025-59485-9.

477

478